Supplement of Atmos. Chem. Phys., 20, 3609–3621, 2020
https://doi.org/10.5194/acp-20-3609-2020-supplement

Atmospheric Chemistry and Physics
Open Access
EGU

Supplement of

Deconvolution of boundary layer depth and aerosol constraints on cloud water path in subtropical stratocumulus decks

Anna Possner et al.

Correspondence to: Anna Possner (apossner@iau.uni-frankfurt.de)

Figures

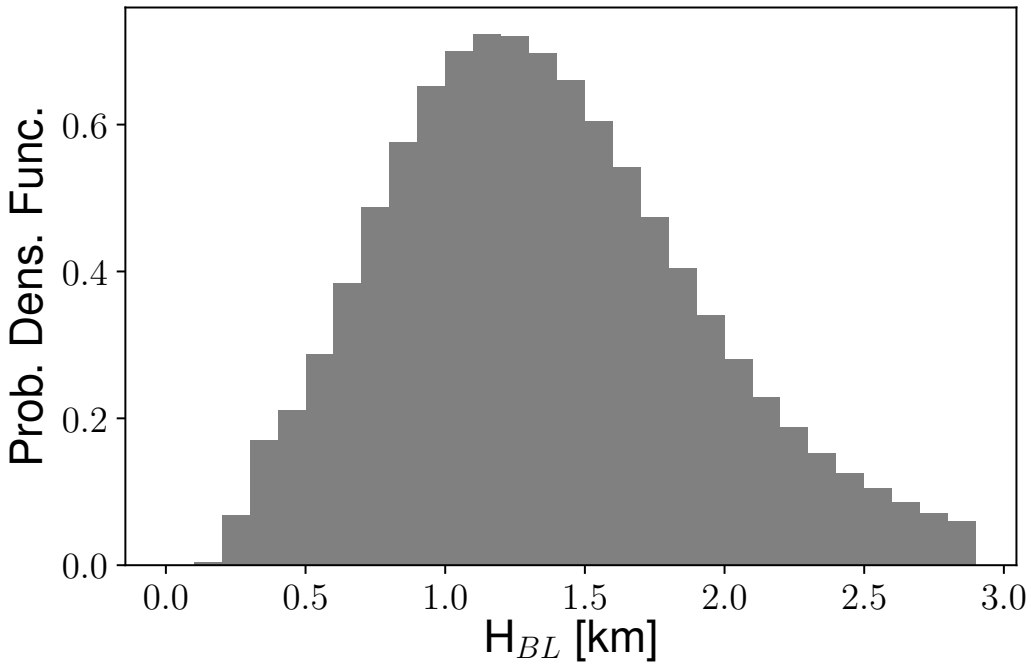

Figure S1. Probability density function of Boundary Layer Height (H_{BL} in Subtropical stratocumulus regions shown in Fig. 2 in main manuscript.

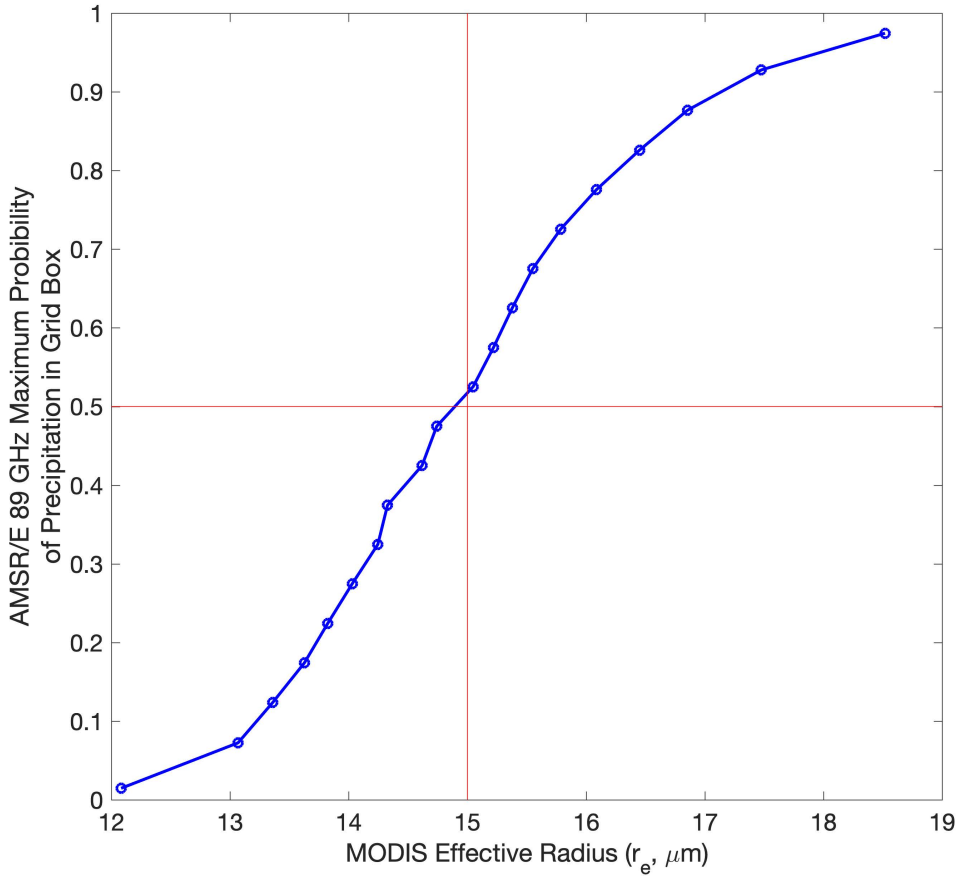

Figure S2. Effective radius (R_{eff}) plotted against precipitation probability at cloud base for all sub-tropical marine stratocumuli. The precipitation probabilities at cloud base were obtained from the Advanced Microwave Scanning Radiometer for (AMSR/E) 89 GHz brightness temperature, for which a retrieval algorithm has been developed based on light rain CloudSat retrievals in collocating regions (*Eastman et al.* [2019]). Only data for the year 2007 are included here for which the precipitation probability retrieval is available.

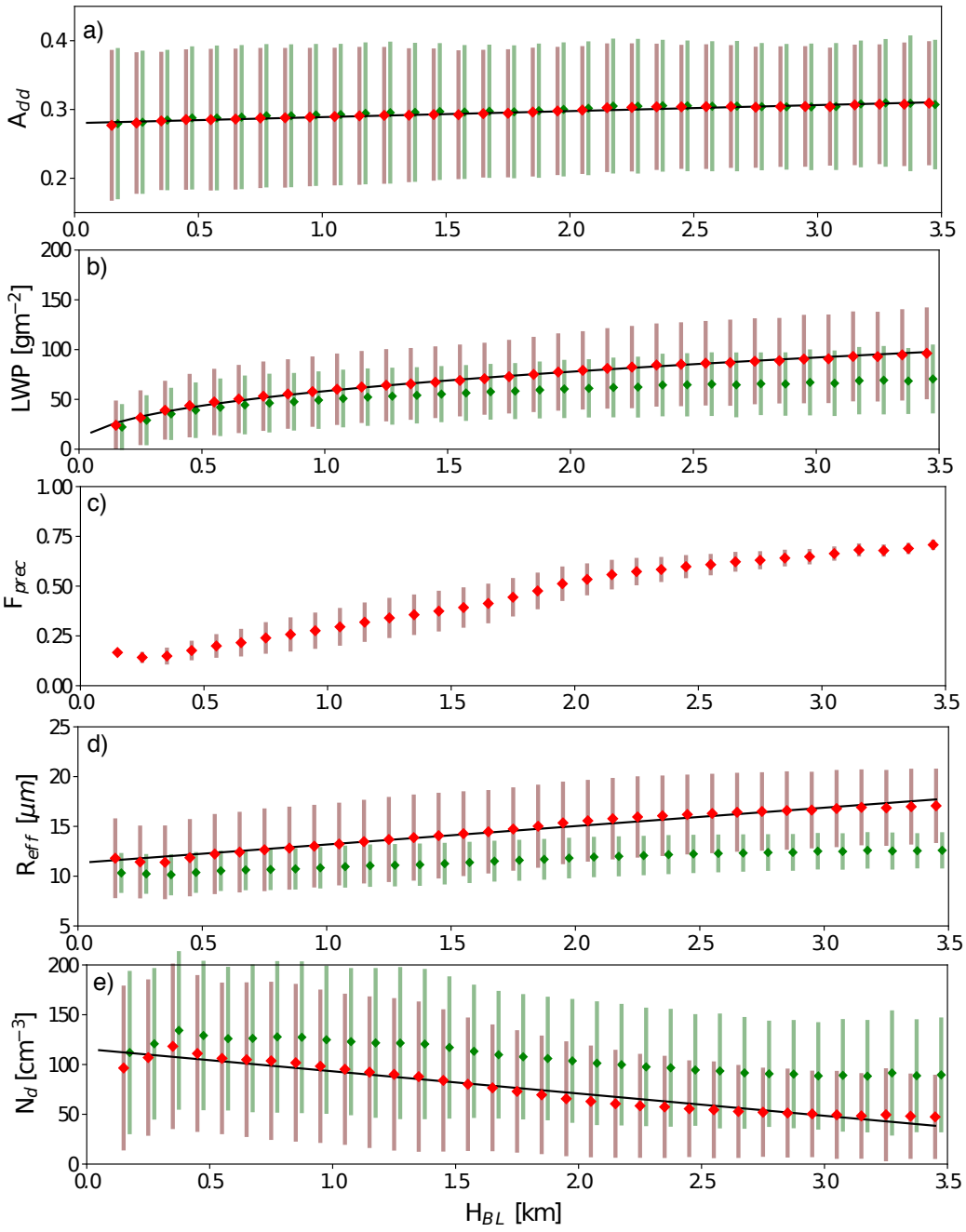

Figure S3. Same as Fig. 3 of manuscript. Scaling relations are shown for all clouds (red) with superimposed fitting lines (black) and non-precipitating clouds (green).

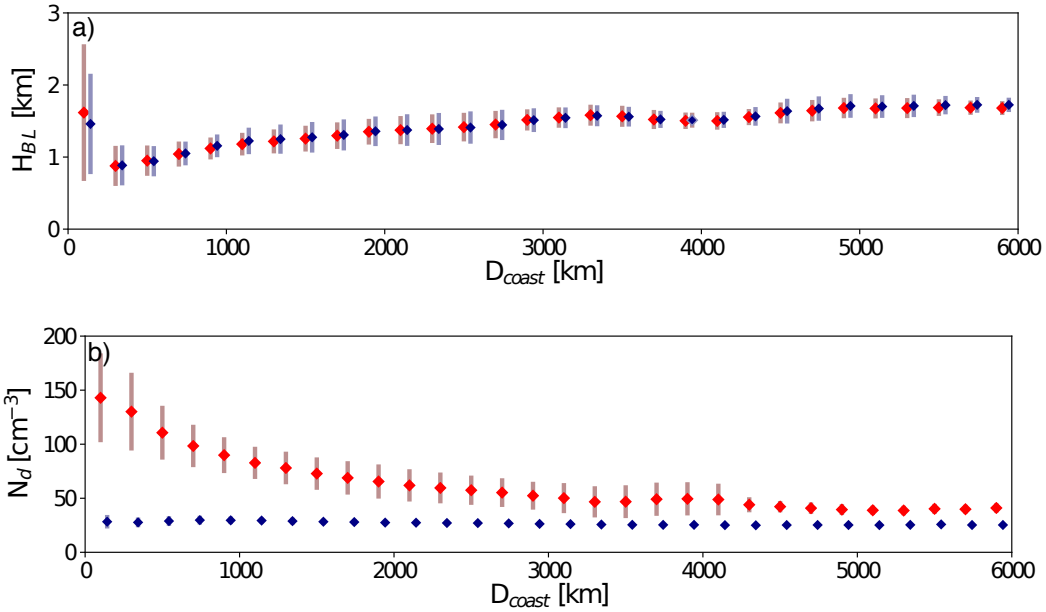

Figure S4. (a) Increase in boundary layer depth (H_{PBL}), and (b) decrease in cloud droplet number concentration (N_d) with increasing distance to the nearest continent. The distance to the nearest shore line is approximated by the distance to the nearest land point at a given latitude (D_{coast}). The mean and standard deviation are computed within each 200 km-wide bin based on the H_{PBL} and N_d climatologies within the Southeast Pacific, Northeast Pacific, and Southeast Atlantic stratocumulus regions depicted in Fig. 2. The relationship for all clouds is shown in red and for precipitating clouds in blue.

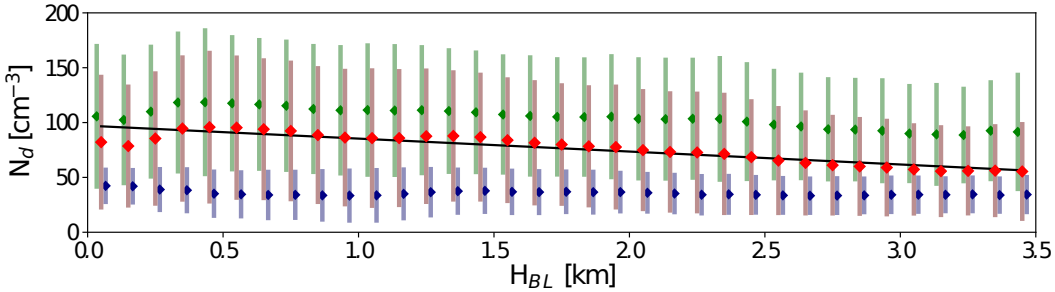

Figure S5. De-seasonalised and de-regionlised N_d climatology against H_{BL}. Markers denote climatological mean and bars denote the standard deviation for all clouds (red), precipitating clouds (blue) or non-precipitating clouds (green).

Quantity	stability		above cloud RH		cloud-base precipitation			all
	stable	non-stable	dry	moist	no-rain	rain		
sample size	1 753 467	276 745	1 688 442	341 770	1 313 803	715 109		2 030 212
$\sigma_{\ln LWP}$	0.01	0.02	0.01	0.02	0.01	0.02		0.006
$\overline{\sigma_{R_{eff}}}$	0.005	0.007	0.05	0.002	0.002	x		0.004
$\overline{\sigma_{N_d}}$	0.01	x	0.02	0.009	0.01	x		0.01
$\overline{\sigma_{A_{cld}}}$	0.001	0.002	0.002	x	0.001	0.002		0.001
						fully	partially	
sample size	1 699 750	225 363	1 662 972	290 586	948 579	279 278	727 614	1 958 215
σ_{lwp} (bivariate)	0.001	0.002	0.001	0.06	0.002	0.004	0.002	0.001
σ_{lwp} (N_d-only)	0.004	0.006	0.006	0.006	0.01	0.04	0.006	0.004

Table S1. This table provides the statistical error (denoted here as σ) of the slopes determined by ordinary least squares regression in Table 1 of the manuscript. The sample size of each regime is included for the first part of this table characterising the PBL depth dependence and the second part separately.